


GLOBAL DISTRIBUTION AND DIVERSITY OF MARINE EUENDOLITHIC CYANOBACTERIA¹

Adam J. Wyness ²

Coastal Research Group, Department of Zoology and Entomology, Rhodes University, Makhanda (Grahamstown), South Africa 6139

School of Biology and Environmental Sciences, University of Mpumalanga, Mbombela, South Africa 1200

Daniel Roush

Center for Fundamental and Applied Microbiomics, Bidesign Institute, Arizona State University, Tempe, Arizona, 85287, USA

and Christopher D. McQuaid

Coastal Research Group, Department of Zoology and Entomology, Rhodes University, Makhanda (Grahamstown), South Africa 6139

Euendolithic, or true-boring, cyanobacteria actively erode carbonate-containing substrata in a wide range of environments and pose significant risks to calcareous marine fauna. Their boring activities cause structural damage and increase susceptibility to disease and are projected to only intensify with global climate change. Most research has, however, focused on tropical coral systems, and limited information exists on the global distribution, diversity, and substratum specificity of euendoliths. This metastudy aimed to collate existing 16S rRNA gene surveys along with novel data from the south coast of South Africa to investigate the global distribution and genetic diversity of endoliths to identify a “core endolithic cyanobacterial microbiome” and assess global diversification of euendolithic cyanobacteria. The cyanobacterial families Phormidiesmiaceae, Nodosilineaceae, Nostocaceae, and Xenococcaceae were the most prevalent, found in >92% of categories surveyed. All four known euendolith clusters were detected in both intertidal and subtidal habitats, in the North Atlantic, Mediterranean, and South Pacific oceans, across temperate latitudes, and within rock, travertine tiles, coral, shell, and coralline algae substrata. Analysis of the genetic variation within clusters revealed many organisms to be unique to substratum type and location, suggesting high diversity and niche specificity. Euendoliths are known to have important effects on their hosts. This is particularly important when hosts are globally significant ecological engineers or habitat-forming species. The findings of this study indicate

high ubiquity and diversity of euendolithic cyanobacteria, suggesting high adaptability, which may lead to increased community and ecosystem-level effects with changing climatic conditions favoring the biochemical mechanisms of cyanobacterial bioerosion.

Key index words: bioerosion; climate change; coralline algae; cyanobacteria; endolith; microbiome; ocean acidification; rocky shore; taxonomy

Abbreviations: ASV, amplicon sequence variants; Gya, billion years ago; HTP, high throughput; SIMPROF, similarity profile permutation test; UBC, unknown boring cluster

Bioerosion by photosynthetic euendolithic (also known as boring) microorganisms causes structural damage to organic carbonate structures, and weathering of rocks in terrestrial, marine, and freshwater environments. Bioerosion also occurs through the actions of heterotrophic microorganisms, as well as sponges, invertebrates, and the vertebrates that feed on them. The process of bioerosion plays an important role in both local (e.g., coral reefs) and global biogeochemical cycles (Schneider and Le Campion-Alsumard 1999, Tribollet 2008, Gleason et al. 2017a, 2017b). Euendoliths are also important primary producers (Tribollet 2008) that contribute significantly to the cycling of nutrients, especially carbon and nitrogen, in nearshore marine waters (Tribollet et al. 2006, Pfister et al. 2010). Euendoliths bore into a wide range of substrata (Ramírez-Reinat and Garcia-Pichel 2012a; Couradeau et al. 2017), but are particularly

¹Received 28 October 2021. Accepted 23 August 2022.

²Author for correspondence: e-mail adamjwyness@hotmail.com
Editorial Responsibility: J.L. Collier (Associate Editor)

efficacious in carbonate-containing rock and the calcium carbonate exoskeletons of organisms such as mollusks (Kaehler and McQuaid 1999, Ndhlovu et al. 2019), crustacea, echinoderms, and corals (Campion-Alsumard and Hutchings 1995, Pernice et al. 2020). The damage caused by euendoliths weakens the structural integrity of the substratum, which increases the costs of repair and maintenance for host organisms (Kaehler and McQuaid 1999, Day et al. 2000, Zardi et al. 2009, Ćurin et al. 2014) and increases erosion rates of carbonate coastlines (Donn and Boardman 1988). For living organisms, boring also increases the chance of lethal damage from shell collapse, predation, or physical impacts (Webb and Korubel 1994, Kaehler and McQuaid 1999), as well as vulnerability to disease (Gleason et al. 2017a). The euendolithic lifestyle is found across a wide range of organisms, including fungi, green and red algae, cyanobacteria, and sponges (Gektidis et al. 2007, Cockell and Herrera 2008, Schönberg and Wisshak 2012, Murphy et al. 2016, Gleason et al. 2017b). The cyanobacteria include numerous species of euendoliths such as *Hormathonema* sp., *Hyella* sp., *Mastigocoleus testarum*, and *Plectonema terebrans*, frequently occurring at high abundances on limpets, mussels, rocks, and experimental carbonate blocks (Gektidis et al. 2007, Prusina et al. 2015, Ndhlovu et al. 2019). Their boring lifestyle may provide them with several ecological advantages including protection from environmental extremes, excessive ultraviolet light, abrasive detachment from substrata, grazing and predation, and increased access to nutrients (Guida et al. 2017).

Recent research has suggested that the euendolithic lifestyle evolved as an alternative carbon acquisition mechanism during a time when dissolved inorganic carbon was less readily available for autotrophy (Guida et al. 2017). Euendoliths have been observed to be organically preserved in limestones from 700–800 Mya (Knoll et al. 1986), and there is evidence of their presence possibly as long ago as ~3.4 Gya (Banerjee et al. 2006, Brasier et al. 2006). In the present day, euendoliths are ubiquitous, and they, along with other endoliths (chasma- and crypto-endoliths; organisms that exploit rock surfaces, fissures, spaces in porous rocks as well as euendolithic excavations) have been observed in many ecosystems and habitats around the globe (Golubic et al. 1981).

Endoliths are of particular interest in marine systems because their bioerosive ability is likely to increase with increasing ocean acidification and temperatures through global climate change, which could have devastating impacts on the fitness and mortality of ecologically important calcifying organisms and ecosystems (Zardi et al. 2009, Marquet et al. 2013). These include coral reefs (Pernice et al. 2020), coralline algae, and bivalve beds (Orr et al. 2005, Garcia-Pichel et al. 2010, Diaz-Pulido

et al. 2011), in addition to carbonate coastlines important to the tourism industry in places such as Menorca (Roush et al. 2018), the Caribbean archipelago (Donn and Boardman 1988, Cambers 2005), and carbonate beaches in Australia (Short 2001). There is a wealth of research on the detrimental effects of ocean acidification on the biology of calcifying fauna (Orr et al. 2005, Gazeau et al. 2007, Melzner et al. 2011, Rodolfo-Metalpa et al. 2011, Stumpp et al. 2011), but little research exists on how on how calcium carbonate degrading organisms will exacerbate erosion rates, threatening natural ecosystems (De'ath et al. 2009, Tribollet et al. 2009, Diaz-Pulido et al. 2011) and commercial bivalve aquaculture (Zardi et al. 2009).

Ocean acidification facilitates chemical erosion by euendoliths; as lower pH reflects a higher concentration of carbonic acid in the surrounding water, resulting in increased spontaneous dissolution of calcium carbonate, in addition to “softening” the exposed surfaces of calcium carbonate structures, thus enabling more effective mechanical erosion (Tribollet et al. 2009, Schönberg et al. 2017). Higher dissolution rates of calcium carbonate decrease the energy expenditure required to pump calcium ions away from the substrate, facilitating euendolithic bioerosion of calcium carbonate (Garcia-Pichel et al. 2010, Ramírez-Reinat and Garcia-Pichel 2012a; Guida and Garcia-Pichel 2016). Increasing ocean acidification also affects calcifying organisms directly as the saturation state of calcium carbonate decreases (Caldeira and Berner 1999, Hurd et al. 2020, Zhao et al. 2020), making it metabolically more difficult to mineralize. The greatest pH changes are expected in surface waters (Caldeira and Wickett 2003), putting shallow water and intertidal organisms, especially at risk. For example, euendolithic infestation can damage large proportions of populations of mollusks such as the mussels *Mytilus galloprovincialis* (Marquet et al. 2013, Ndhlovu et al. 2019) and *Modiolus barbatus* (Ćurin et al. 2014), and the limpet *Patella rustica* (Prusina et al. 2015). In fact, euendoliths can be responsible for up to 60% of total mortality in mussel populations through shell collapse by bioerosion (Kaehler and McQuaid 1999, Zardi et al. 2009, Ndhlovu et al. 2019).

To understand the ramifications of global climate change on the interactions of euendoliths, calcifying organisms and the ecosystems that rely upon them requires an understanding of the distribution, diversity, and function of euendoliths, endoliths, and facilitating organisms. In this study, a meta-analysis approach was used to examine the prevalence and diversity of euendolithic cyanobacteria, and at the same time, apply new molecular methods to analyze euendolithic species. All available 16S rRNA gene amplicon sequencing data from relevant carbonate endolith microbiome studies were re-examined, along with new sequencing data collected on the

coast of South Africa for this study. This metastudy had three specific objectives: to (i) identify a core endolithic microbiome of cyanobacteria across calcium carbonate structures; (ii) examine the presence of euendoliths across ecosystems, including habitat, substrata, and geographic location; and (iii) investigate the genetic diversity within known euendolith clades to determine the ubiquity of known euendolithic organisms.

MATERIALS AND METHODS

Sample collection. Live organisms (the mussel *Perna perna*, the barnacle *Octomeris angulosa*, the whelk *Burnupena lagenaria*, and the limpet *Scutellastra cochlear*) and rock chips were collected from the intertidal rocky shore at Morgans Bay (32°42'39.2" S 28°20'23.1" E) and Cannon Rocks (33°45'06.8" S 26°32'41.6" E) on the south coast of South Africa during September 2019. Samples were milled to create a fine dust using a flame-sterilized Dremel (WI, USA) 4.4 mm diamond wheel point bit, and the resulting fine particulate material weighed into 1.5 mL microcentrifuge tubes. The most eroded section of shells (typically the apex) was used for extraction.

16S rRNA gene library preparation and Illumina sequencing. DNA extractions were performed by incubating samples in 487.5 μ L concentrated lysis buffer (final concentrations: 50 mM Tris-HCl pH 8.0, 100 mM EDTA pH 8.0, 100 mM NaCl, 0.5% SDS) and 12.5 μ L of Proteinase K (20 mg \cdot mL⁻¹) at 55°C for 12 h. DNA was then extracted following a standard phenol/chloroform/isoamylalcohol (25:24:1) extraction method (Hogan et al. 1986, Geist et al. 2008).

Extracted DNA was quantified (NanoDrop 2000, Thermo Scientific) and extractions from the six individuals of each species for each site pooled in equal concentrations. The 16S rDNA v3- v4 region was amplified under the following PCR conditions: 341f (5'-TCGTCGGCAGCGTCAGATGTGTA TAAGAGACAGCCTACGGGNGGCWGCAG) and 805r (5'-GTCTCGTGGGCTCGGAGATGTGTATAAGAGACAGGACTA CHVGGGTATCTAATCC; Klindworth et al. 2013), 25 ng of template DNA (pooled), 5 pmol of each primer, and 0.5 units of Phusion Flash High-Fidelity taq polymerase mastermix (ThermoFisher Scientific) in a 25 μ L reaction under the following conditions: Initial denaturation at 98°C for 10 s, followed by 25 cycles of 98°C for 5 s, 55°C for 10 s, 72°C for 30 s, and a final extension at 72°C for 60 s.

PCR product clean-up was performed using 20 μ L of AMPure XP beads (Agencourt, Beckmann Coulter) per sample, 2 \times 200 μ L washes of 80% ethanol, and resuspended in 50 μ L of 10 mM Tris pH 8.5 buffer. Illumina sequencing adapters (Nextera XT Index Kit, Illumina) were attached using 20 ng of template DNA, 4 μ L of index primer, and 0.8 units of KAPA HiFi HotStart ReadyMix in a 40 μ L reaction under the following conditions: Initial denaturation at 95°C for 3 min, followed by 8 cycles of 95°C for 30 s, 55°C for 30 s, 72°C for 30 s, and a final extension at 72°C for 5 min. Final PCR products were cleaned using 56 μ L of AMPure XP beads, 2 \times 200 μ L washes of 80% ethanol, and resuspended in 25 μ L of 10 mM Tris pH 8.5 buffer. The prepared library was pooled at a concentration of 4 nM and sequenced on a MiSeq (Illumina) using the 600-cycle MiSeq reagent kit v3 (Illumina) with a 5% spike-in of pre-prepared PhiX sequencing control v3 library (Illumina). Sequencing was performed by the Aquatic Genomics Research Platform at the South African Institute for Aquatic Biodiversity (SAIAB, Grahamstown, South Africa). Sequence data were deposited

and are publicly available in the NCBI Sequence Read Archive (SRA) under the BioProject ID PRJNA634631.

Metastudy data retrieval. A "Web Of ScienceTM" advanced search was performed with the terms: TS = ((biofilm OR endolith* OR microbiota OR epilith*) AND (16S OR metabarcod* OR sequenc* OR amplicon) AND (intertidal OR shell OR coral* OR rock OR calcium OR calcareous OR carbonate OR exoskeleton)). The initial search yielded 1239 results. Studies were filtered by study title and abstract where studies using sequencing of marine calcium carbonate structures were included ($n = 226$). A final filter of studies was performed with studies included only if they extracted DNA from the whole structure rather than swab or tissue only (therefore including euendolithic bacteria), and the data were readily available, correctly formatted and with sufficient accompanying metadata. This resulted in 16 Sanger sequencing studies and 17 high-throughput sequencing (HTP) studies to be included in this metastudy (Table 1). The samples from which data were obtained for this study, and the method of DNA extraction for samples collected for this study included the whole skeleton or shell; therefore, epilithic and chasmoendolithic population will be included. Hypotheses 2 and 3 were limited to previously determined "euendolith" clusters in order to focus analyses on euendolith populations.

Bioinformatic analysis. Sequence data were retrieved using the SRA toolkit (SRA Toolkit Development Team 2020) and imported into QIIME2 v2020.2 (Bolyen et al. 2019) alongside the novel sequence data obtained during this study. After adaptor-trimming and read-joining (if applicable), HTP sequences were quality filtered, chimeras removed, and the data denoised using DADA2 (Callahan et al. 2016) and Deblur (Amir et al. 2017) pipelines for pyrosequenced and Illumina sequenced samples, respectively. All sequences were then allocated to taxa using the SILVA 132 database (Quast et al. 2013) using the Blast+ consensus classifier (Camacho et al. 2009). Taxa that were of the phylum Cyanobacteria were included, and chloroplasts excluded.

Cluster and SIMPROF analyses were used to generate dendrograms for the core cyanobacterial microbiome using PRIMER6 (Clarke and Gorley 2006) with group average clustering and 1000 permutations on a presence/absence Sørensen resemblance matrix of sequences that were allocated to at least Order level. For the identification of sequences that matched to known euendolith clusters, 16S rRNA sequences were placed into a reference tree following the Cydrasil 2.0 protocol (Roush et al. 2021). The placed sequences were visualized and manipulated within iTOL v4 (Letunic and Bork 2019) to extract sequences that were placed with a likelihood ratio > 0.7 within known euendolith clusters (Roush and Garcia-Pichel 2020).

To analyze the genetic diversity of Amplicon Sequence Variants (ASVs) within clusters, all sequences were aligned, and a ~211 bp section (16S rRNA position ~557–768) of the V3–V4 region of the 16S rRNA gene extracted as this section was fully contained within 3211 of the total of 4051 sequences. Sequences that placed within each known cluster were extracted and aligned using MAFFT v7 (Katoh and Standley 2013), and a maximum likelihood tree was built with RaxML v8 with the GTRGAMMA substitution model and 1000 bootstraps (Price et al. 2010). Trees were visualized and manipulated within MEGA 7.0 (Kumar et al. 2016) and Figtree V1.4.4 (Rambaut 2012).

RESULTS

The core cyanobacterial microbiome of calcium carbonate structures. To analyze the presence and distribution

TABLE 1. Studies, citations, and relevant sample or sequence (depending on sequencing type) accession numbers and metadata for the samples included in the meta-analysis.

Author (Year)	Sample/Read Accession	Country	Region	Ocean	Latitude	Longitude	Host	Habitat	Sequencing Type
Aldred and Nelson (2019)	PRJNA524314	England	Northwest	North Sea	55°02' N	1°25' W	Barnacle	Intertidal	HTP
Arfken et al. (2017)	PRJNA385615	USA	North Carolina	North Atlantic	34°42' N	76°45' W	Shell	Intertidal	HTP
Brito et al. (2012)	HQ832901	Portugal	Molodo	North Atlantic	41°50' N	8°32' W	Shell	Intertidal	Single read
Chacón et al. (2006)	DQ380390 - DQ380404	Puerto Rico	Cayos De Barca	North Atlantic	17°55' N	66°15' W	Shell, Coralline algae and Rock	Intertidal	Single read
Cleary et al. (2019)	PRJNA382576	Taiwan	Penghu County	North Pacific	23°31' N	119°36' E	Barnacle, Chiton, Coral, Echinoderm, Mussel, Shell	Subtidal	HTP
Couradeau et al. (2017)	KT972744 - KT981874; KX388631; KX388632; KX388633	Puerto Rico	Isla de Mona	North Atlantic	18°08' N	67°88' W	Rock and Shell	Intertidal	Single read
Diaz et al. (2013)	JQ917486 - JQ917719	Bahamas	Bahamas Archipelago	North Atlantic	23°53' N	75°22' W	Rock	Subtidal	Single read
Foster et al. (2009)	EU248965 - EU249128; FJ373355 - FJ373445	Bahamas	Highborne Cay	North Atlantic	24°43' N	76°49' W	Stromatolite	Subtidal	Single read
Godoy-Vitorino et al. (2017)	PRJNA379103	Puerto Rico	Isla Palominos	North Atlantic	18°21' N	65°34' W	Coral	Subtidal	HTP
Goldsmith et al. (2019)	MK175495 - MK176300	USA	Rhode Island	North Atlantic	41°37' N	71°20' W	Coral	Subtidal	Single read
Havemann and Foster (2008)	EU1917948 - EU1918121	Bahamas	Highborne Cay	North Atlantic	24°43' N	76°49' W	Stromatolite	Intertidal	Single read
Kimes et al. (2013)	JQ514788 - 7143	Puerto Rico	La Panguera	North Atlantic	17°56' N	67°02' W	Coral	Subtidal	Single read
Li et al. (2013)	PRJNA196815	China	Hainan Province	North Pacific	18°13' N	109°28' E	Coral	Subtidal	HTP
Marcelino et al. (2017)	PRJNA390873	Papua New Guinea	D'Entrecasteaux Isl.	South Pacific	9°41' S	150°48' E	Coral	Subtidal	HTP
Marcelino and Verbruggen (2016)	PRJNA319725	Various	Various	Various	-	-	Coral, Coralline algae, Rock	Subtidal	HTP
Pfister et al. (2014)	PRJEB18565	USA	Washington	North Pacific	48°32' N	124°74' E	Shell	Intertidal	HTP
Pollock et al. (2018)	PRJEB28183	Australia	Various	Various	-	-	Coral	Subtidal	HTP
Quééré et al. (2019)	PRJNA524010	France	Banyuls-sur-Mer	Mediterranean Sea	42° N	3° E	Coralline algae	Subtidal	HTP
Ramirez-Reinat and Garcia-Pichel (2012a, 2012b)	JN810702 - JN810746	Various	Various	Various	-	-	Coralline algae	Intertidal	Single read
Ramirez-Reinat and Garcia-Pichel (2012a, 2012b)	HQ906640 - HQ906642	Puerto Rico	Cabo Rojo	North Atlantic	17°56' N	67°11' W	Shell	Intertidal	Single read
Roush et al. (2018)	PRJNA396581	Menorca	Several	Mediterranean Sea	39°58' N	4°5' E	Rock	Intertidal	HTP
Roush et al. (2020)	PRJNA596277; PRJNA603780	Puerto Rico	Isla de Mona	North Atlantic	18°08' N	67°88' W	Rock, Travertine tiles	Intertidal	HTP
Rubio-Porlillo et al. (2016)	KU936838 - KU936871	Spain	Alicante	Mediterranean Sea	38°13' N	0°28' W	Coral	Subtidal	Single read
Rubio-Porlillo et al. (2016)	PRJNA315808	Spain	Alicante	Mediterranean Sea	38°13' N	0°28' W	Coral	Subtidal	HTP
Schöttner et al. (2011)	FR851476 - FR851758	Jordan	Red Sea	Indian Ocean	29°27' N	34°58' E	Rock	Subtidal	Single read
Sharp et al. (2017)	PRJNA380119	USA	Rhode Island	North Atlantic	41°28' N	71°21' W	Coral	Subtidal	HTP
Sunagawa et al. (2009)	FJ202063 - FJ203662	Panama	Bocas del Toro	North Atlantic	9°15' N	82°07' W	Coral	Subtidal	Single read
Sunagawa et al. (2010)	GU117926 - GU119887	Panama	Bocas del Toro	North Atlantic	9°15' N	82°07' W	Coral	Subtidal	Single read
Vijayan et al. (2019)	PRJNA418344	USA	Hawai'i	North Pacific	15°21' N	157°37' W	Polychaete tubes	Subtidal	HTP
Webster et al. (2011)	HMI177481 - HMI178663; HMI177481 - HMI178656	Australia	Great Barrier Reef	South Pacific	18°49' S	147°38' E	Coralline algae	Subtidal	Single read
Wenzel et al. (2018)	PRJNA438614	Scotland	North East	North Sea	57°07' N	2°03' W	Isopods	Intertidal	HTP
Williams et al. (2015)	KT962875 - KT962900	Thailand	Ko Phuket	Indian Ocean	7°30' N	98°25' E	Coral	Intertidal	Single read
This Publication	PRJNA634631	South Africa	East Cape	Indian Ocean	33°08' S	27°44' E	Rock, Shell	Intertidal	HTP

Categories of latitude, ocean, host substrata, and habitat were those used for the analysis of the distribution of cyanobacteria and eucenololiths.

of all cyanobacterial taxa among systems, sequences were collapsed to the family-level automated phylogenetic placements as designated by the SILVA database (referred to hereon as “SILVA families”). Family level was selected despite there being some physiological differences among species at this taxonomic rank, as it allowed for good differentiation among systems and retaining information on potential physiological effects while avoiding speculation on organism physiology at the species level. The number of studies representing each category was not equal, and several categories were included for which only one appropriate study existed; these included the South Atlantic, echinoderms, isopods, chitons and polychaete tubes, and travertine terrestrially derived limestone predominantly comprised of calcium carbonate in this case placed in marine systems for experimental investigation of euendolithic activity (Roush and Garcia-Pichel 2020). Their inclusion did not, however, appear to influence the overall findings. Rarefaction curves of observed ASVs and number of samples against sequencing depth showed that the asymptote of ASV richness was reached for all categories; therefore, the cause of the trends observed should not be attributed to the sampling effort (Fig. S1 in the Supporting Information). Importantly, as for all ecological studies, nondetection of families does not necessarily indicate their absence.

The methods of DNA extraction for samples included from other studies, and the samples collected for this study include the whole shell; therefore, the cyanobacterial communities reported in “The core cyanobacterial microbiome of calcium carbonate structures” section in the Results include all lithobionts, rather than allowing for the focus on euendoliths. “Global distribution of known euendolithic cyanobacteria” section extracts data only on previously identified euendolithic groups of cyanobacteria to focus on their distribution.

Habitat: A higher number of cyanobacterial SILVA families were detected in intertidal samples than subtidal samples, with all families observed in subtidal samples also being observed in intertidal samples, with the exception of the Prochloraceae, an abundant and important group of marine primary producers (Partensky et al. 1999; Fig. 1). The Thermosynechococcaceae, Rubidibacteraceae, and Limnotrichaceae were observed in intertidal samples but not the subtidal.

Substrata: Cyanobacterial communities were separated into five significantly different substratum groups (SIMPROF; $P < 0.05$; Fig. 2); A, coralline algae, rock, travertine tile, shell (including bivalves and gastropods), and coral; B, barnacle, chiton, and polychaete tubes; and then three hosts were significantly different; C, stromatolite; D, echinoderm, and E, isopod (Fig. 2). Samples from isopods contained no photosynthetic cyanobacteria and were therefore an outlying group. Cyanobacterial

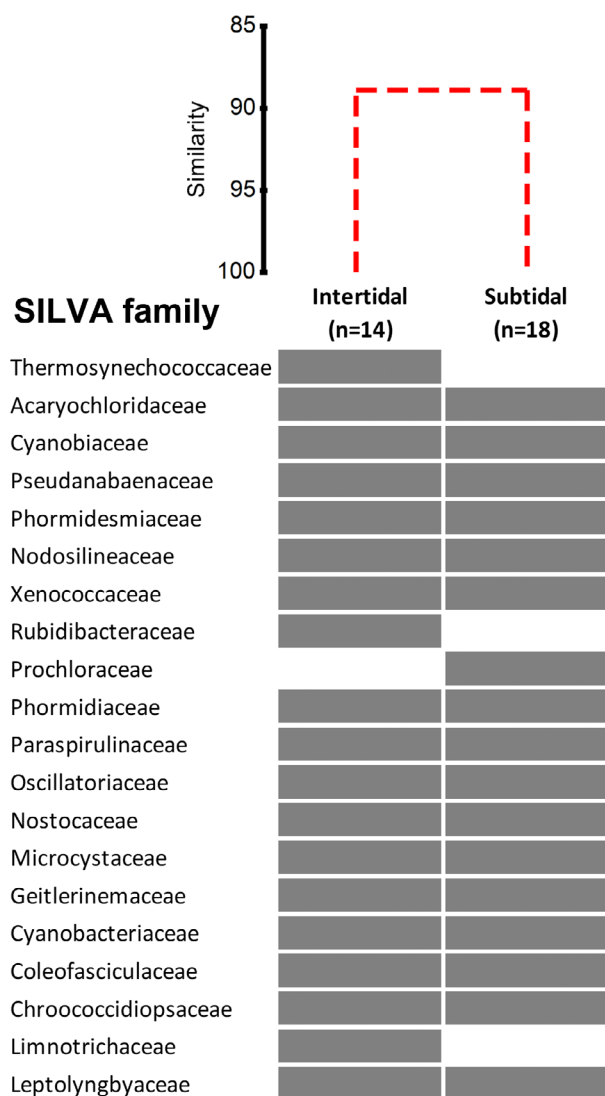


FIG. 1. Distribution of cyanobacterial SILVA families in intertidal and subtidal habitats using 16S rRNA sequence data from 32 previously published studies and novel data collected for this study. Most cyanobacterial families are ubiquitous between intertidal and subtidal locations. Shaded cells indicate presence, and n = the number of unique studies. Dendrogram represents the similarity of communities between habitats using cluster analysis with SIMPROF analysis. Dotted branches indicate a nonsignificant difference between nodes in the SIMPROF analysis. [Color figure can be viewed at wileyonlinelibrary.com]

communities of echinoderms and stromatolites were the least similar to the other substrata (SIMPROF; 44.53% similarity; Pi 6.45, $P < 0.001$, and 59.87%; Pi 4.66 $P < 0.001$ for echinoderms and stromatolites, respectively), with a lower number of detected SILVA families (8 of 20 assigned families). The main groups to which most hosts belonged (A and B) had a similarity of 68.15% (SIMPROF; Pi 4.14, $P < 0.001$). In terms of a core microbiome, out of the 11 substratum types, the Phormidemiaceae and Xenococcaceae were detected in 10 of the 11 substrata, and the Nodosilineaceae, Cyanobacteriaceae,

and Coleofasciculaceae were detected in 9. In the first group of substrata (A), many families were present in all substratum types (Fig. 2), including the Phormidesmiaceae, Xenococcaeae, Nodosilineaceae, Nostocaceae, and Leptolyngbyaceae, which were also observed in both habitats (Fig. 1). Whereas in group B, there was a lower richness of families, with the Thermosynechococcaceae, Pseudanabaenaceae and several families of the Nostocales being absent.

Latitude: Latitude categories were split into 20-degree sections (Fig. S2 in the Supporting Information). Unfortunately, no samples from extreme latitudes (>69° N or > 50° S) were included in the final analysis. However, samples from the more temperate regions (49° N–30° N, 29° N–10° N, 11° S–30° S and 31° S–50° S) were more similar to each other, than to the coldest (69° N–50° N) and equatorial (9° N–10° S) latitudes (SIMPROF; 54.89% similarity; Pi 8.54, $P < 0.002$; Fig. 3). There were no distinctly different communities among samples, rather the temperate samples contained more SILVA families, with up to 19 of the 20 families for 29° N–10° N, compared with just 5 for 69° N–50° N.

The families that were present across all latitudes however were very similar to those present in the majority of habitat and substrata types, which included the Phormidesmiaceae, Xenococcaeae, Nodosilineaceae, and Nostocaceae.

Ocean: The North Atlantic, Mediterranean, and South Pacific formed a group of oceans that was significantly different from the others (SIMPROF; 73.7% similarity, Pi 5.30, $P = 0.009$) and contained the highest numbers of cyanobacterial SILVA families (Fig. 4). The South Atlantic and the Indian Ocean formed a second group, containing fewer families, notably lacking the Oscillatoriaceae, with the North Pacific and North Sea remaining significantly different from each other and the other oceans (Fig. 4). The Phormidesmiaceae and Nodosilineaceae of the Phormidesmiales, and the Xenococcaeae and Nostocaceae of the Nostocales were detected across all oceans in addition to almost all other system categories, forming a core cyanobacterial microbiome.

Global distribution of known euendolithic cyanobacteria. In a study of euendolith colonization dynamics on travertine tiles, Roush and Garcia-Pichel (2020)

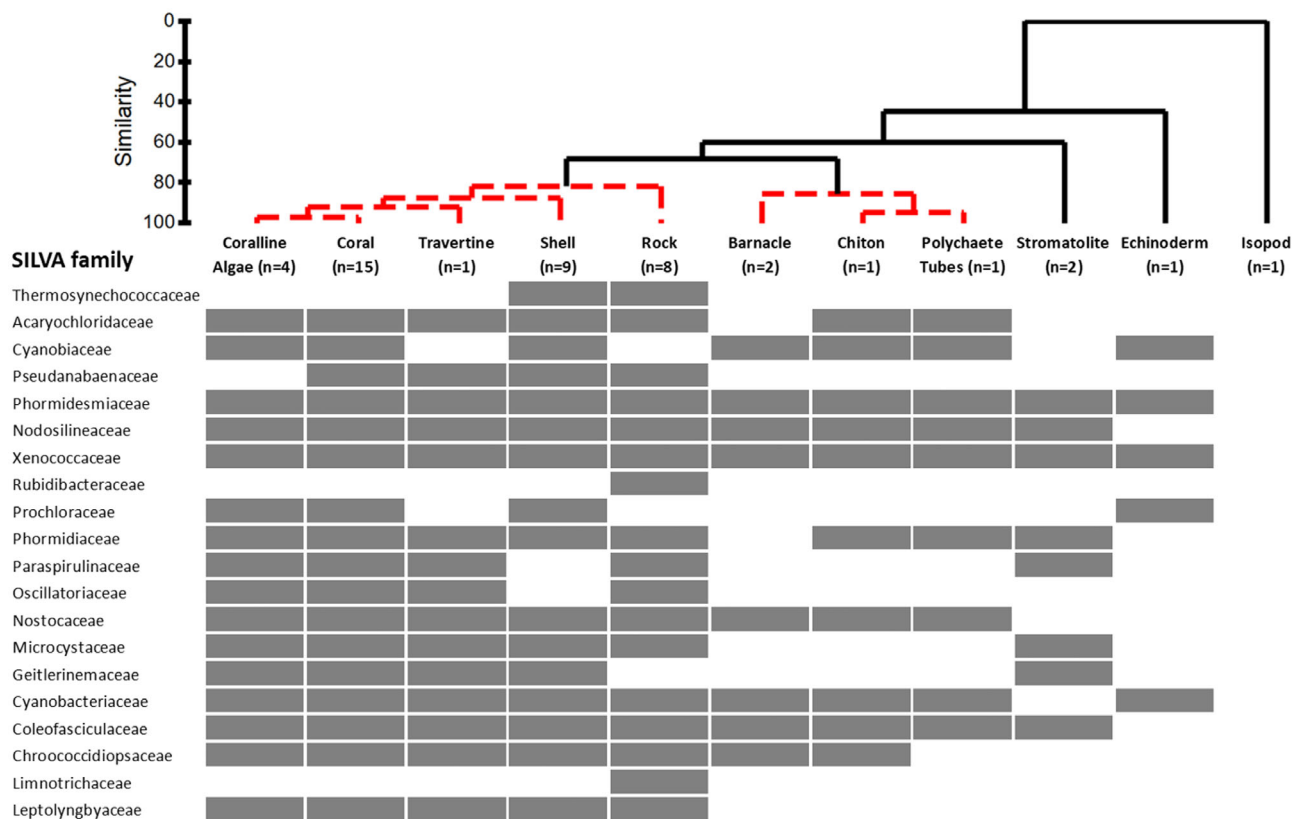


FIG. 2. Distribution of cyanobacterial SILVA families across host substrata using 16S rRNA sequence data from 32 previously published studies and novel data collected for this study. Cyanobacterial families on substrates clustered into five groups: coralline algae, coral, travertine, shell, and rock, and barnacles, chitons, and polychaetes, with Stromatolites, Echinoderms being significantly different from all other substrata. Shaded cells indicate the presence, and n = the number of unique studies. Dendrogram represents the similarity of communities between host substrata using cluster analysis and SIMPROF analysis. Dotted branches indicate a nonsignificant difference between nodes in the SIMPROF analysis. [Color figure can be viewed at wileyonlinelibrary.com]

categorized four main clusters of true euendolithic cyanobacteria. These were used for this study to isolate only euendoliths for examination of their geographic and habitat distribution. Briefly, Cluster 1 is a cluster of *Leptolyngbya*-like cyanobacteria. Cluster 2 contains the Pleurocapsales. Cluster 3 contains ASVs similar to *Mastigocoleus testarum*, a well-studied model organism for euendoliths (Garcia-Pichel et al. 2010). A novel cluster of unknown boring euendoliths, the Unknown Boring Cluster (UBC) was identified as a key pioneer group most closely related to *Stanieria* sp.

All of the clusters were present in both intertidal and subtidal habitats, and on rock, travertine, coral, shell, and coralline algae substrata, with only the *Mastigocoleus testarum* cluster absent from stromatolites (Fig. 5). More than one cluster was absent from chitons, polychaete tubes, and echinoderms, and the UBC was often only present in categories where all other clusters were present. However, all

categories across all systems that contained cyanobacteria contained ASVs that were successfully allocated to a known euendolith cluster. No known euendoliths were detected on isopods, though this was limited to a single study.

All clusters were detected at the temperate latitudes of 49° N–10° N and 31° S–50° S. The UBC was notably absent from 9° N–30° S. The *Leptolyngbya*-like and pleurocapsalean clusters were detected in all oceans, with the *Mastigocoleus testarum*-like being absent only from the North Sea. The UBC however was only present in the North Atlantic, Mediterranean, and South Pacific. Over all categories, the *Leptolyngbya*-like cluster was the most common, detected in 25 of the total 26 categories, followed by the Pleurocapsalean cluster with 21, the *M. testarum*-like cluster with 20, and the UBC with 14.

Genetic diversity within known euendolith cyanobacterial clades. The *Leptolyngbya*-like cluster was the largest

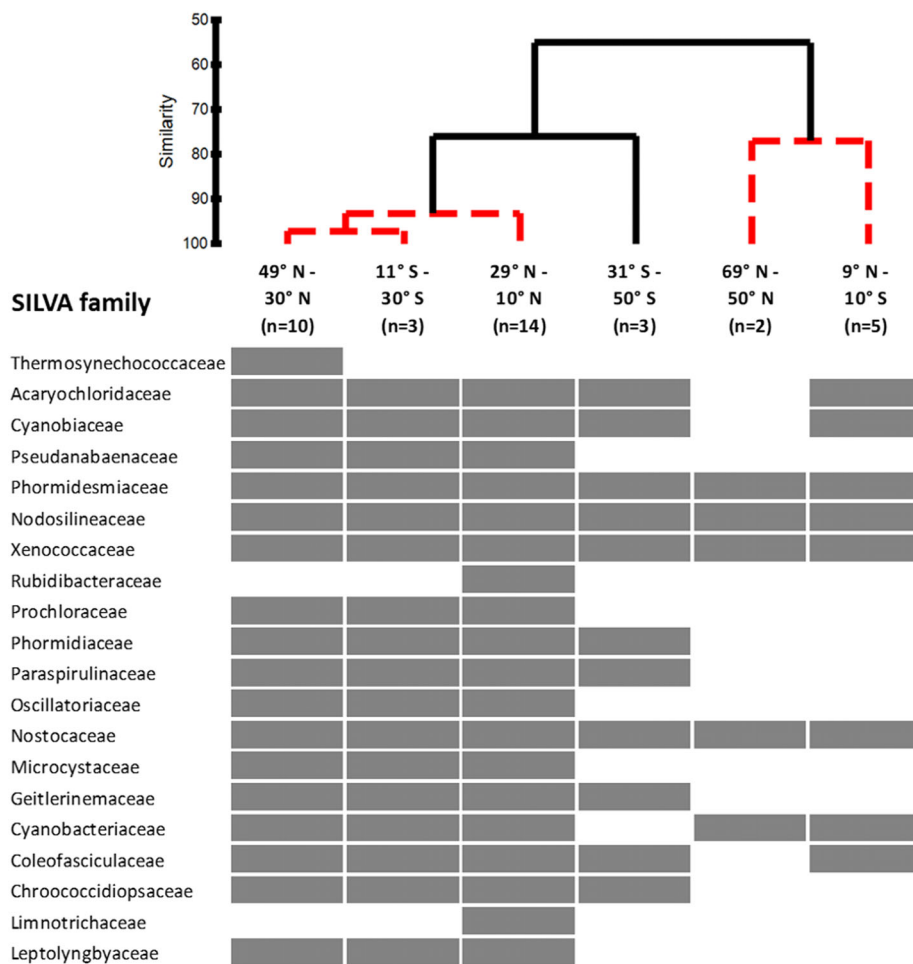


FIG. 3. Distribution of cyanobacterial SILVA families across latitude categories using 16S rRNA sequence data from 32 previously published studies and novel data collected for this study. Cyanobacterial families of temperate regions appeared to cluster together. Shaded cells indicate the presence, and n = the number of unique studies. Dendrogram represents the similarity of communities between latitude categories using cluster analysis and SIMPROF analysis. Dotted branches indicate a nonsignificant difference between nodes in the SIMPROF analysis. [Color figure can be viewed at wileyonlinelibrary.com]

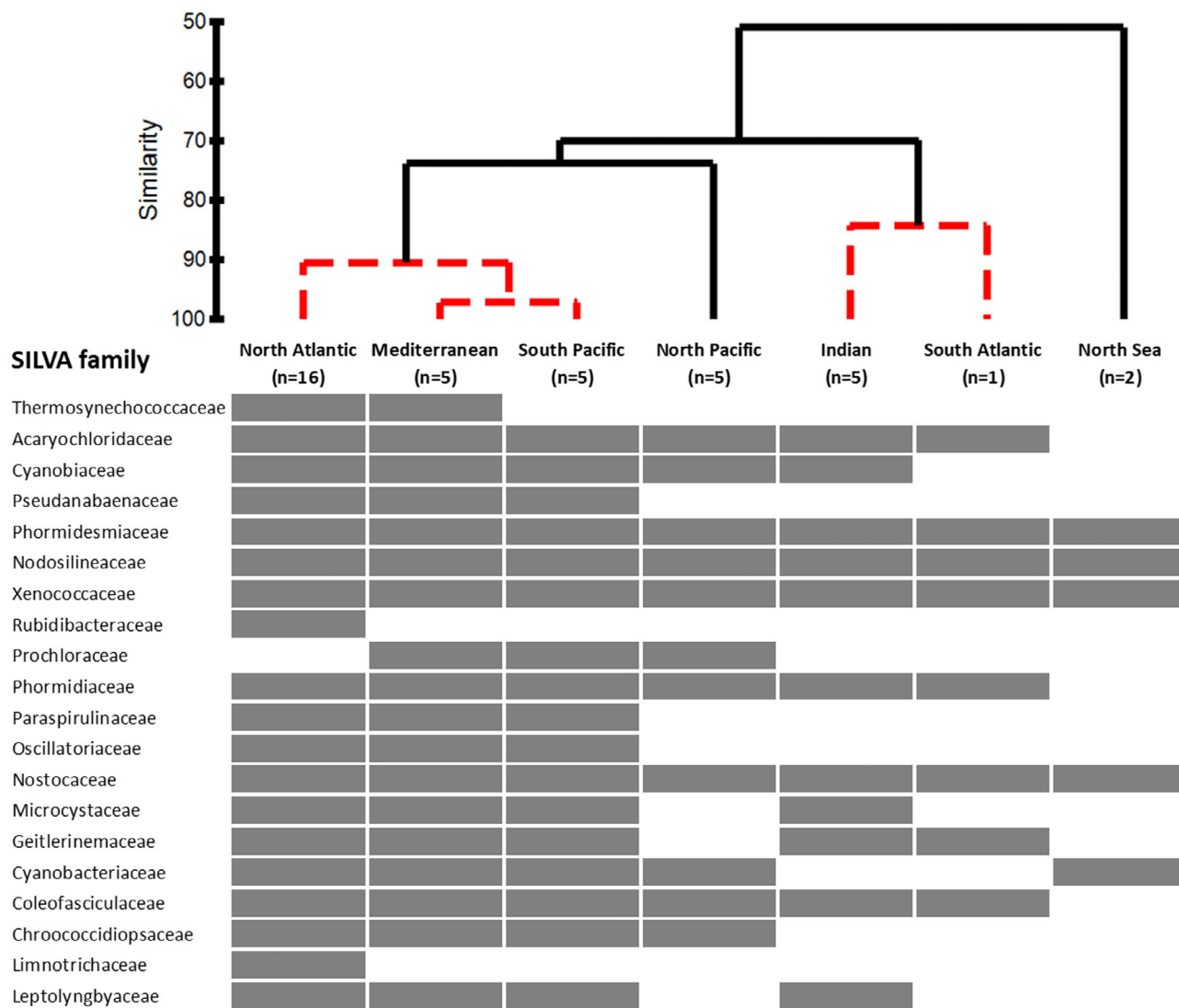


FIG. 4. Distribution of cyanobacterial SILVA families across oceans categories using 16S rRNA sequence data from 32 previously published studies and novel data collected for this study. Similarly, to the latitude categories, cyanobacterial families did not appear to cluster based on ocean connectivity. Shaded cells indicate the presence, and *n* = the number of unique studies. Dendrogram represents the similarity of communities between oceans using cluster analysis and SIMPROF analysis. Dotted branches indicate a nonsignificant difference between nodes in the SIMPROF analysis. [Color figure can be viewed at wileyonlinelibrary.com]

euendolith cluster with 237 ASVs comprising a total of 335 placed sequences, followed by the Pleurocapsalean cluster with 78 ASVs and 147 total sequences. The *Mastigocoleus testarum*-like cluster and the UBC had a similar total number of sequences with 104 and 109, respectively; however, the UBC was aggregated into 20 unique ASVs, whereas the *M. testarum*-like cluster contained 45. The majority of ASVs of the *Leptolyngbya*-like cluster were found only intertidally. Where present, subtidal ASVs were closely clustered and found on more substrata and at more geographic locations than intertidal ASVs (Fig. S3 in the Supporting Information). The majority of *Leptolyngbya*-like ASVs were from the North Atlantic from rock and travertine with sequences from coral, shell, and other locations interspersed. There were,

however, several distinct branches that contained ASVs from a range of locations.

The majority of ASVs belonging to the Pleurocapsalean cluster were found intertidally. Where present, subtidal ASVs were closely related and almost always detected in corals (Fig. S4 in the Supporting Information). Only three ASVs were detected in stromatolites, with two of them being closely related. As with the ASVs in the *Leptolyngbya*-like cluster, some branches appeared to be conservative in their distribution, being limited to only the North Atlantic, whereas some branches were more widely distributed.

The majority of the ASVs allocated to the *Mastigocoleus testarum*-like cluster were found on rocks and travertine, intertidally. Subtidal ASVs were often

found in pairs adjacent to each other, rather than interspersed (Fig. S5 in the Supporting Information). Similarly, ASVs detected in shells were more closely related despite often being detected in geographically different areas, whereas ASVs detected on corals were not closely related and were spread more evenly throughout the phylogenetic tree.

The UBC formed the smallest group of euendoliths detected, with relatively few nucleotide substitutions per site compared with the other clusters (Fig. 6) in addition to several ASVs that contained many sequences from several studies, suggesting lower genetic diversity among ASVs within this group. This small cluster of euendoliths was distributed among fewer categories than other clusters; however, there was a relatively clear structure to the phylogeny of the detected ASVs. The branch annotated UBC:A was almost exclusively detected in intertidal travertine

and rock samples, from the Roush et al. (2020) study that originally detected the cluster (Roush and Garcia-Pichel 2020), whereas the majority of ASVs were detected subtidally or both intertidally and subtidally. Only one ASV was detected on coral (UBC:B), and it was not detected in any other samples.

DISCUSSION

Core cyanobacterial community. The first objective of this study was to identify whether there was a core microbiome of lithobiontic cyanobacteria across calcium carbonate structures in different substrata and geographical systems. The Phormidiales and Nodosilineaceae of the Phormidiales, the Xenococcales, Nostocales, and Chroococcales of the Nostocales and the Leptolyngbyales formed a group of

		Number of	Cluster	Cluster	Cluster	UBC
		Studies	1	2	3	
Habitat	Intertidal	14				
	Subtidal	18				
Substrata	Rock	8				
	Travertine	1				
	Coral	15				
	Shell	9				*
	Stromatolite	2				
	Chiton	1				
	Echinoderm	1				
	Barnacle	2				
	Isopod	1				
	Coralline Algae	4				
	Polychaete Tubes	1				
Latitude	69° N - 50° N	2				
	49° N - 30° N	10				
	29° N - 10° N	14				
	9° N - 10° S	5				
	11° S - 30° S	3				
	31° S - 50° S	3				
Ocean	North Atlantic	16				
	South Atlantic	1				
	Mediterranean	5				
	North Sea	2				
	North Pacific	5				
	South Pacific	5				
	Indian	5				

FIG. 5. Distribution of previously recognized euendolithic clusters among different habitats, host substrata, latitude categories, and oceans using 16S rRNA sequence data from 32 previously published studies and novel data collected for this study. The UBC only colonizes nonliving substrates, while the three more well-known clusters are more cosmopolitan in their habitats, where n = the number of unique studies and * denotes a study containing those sequences that did not discriminate between dead coral and dead shell.

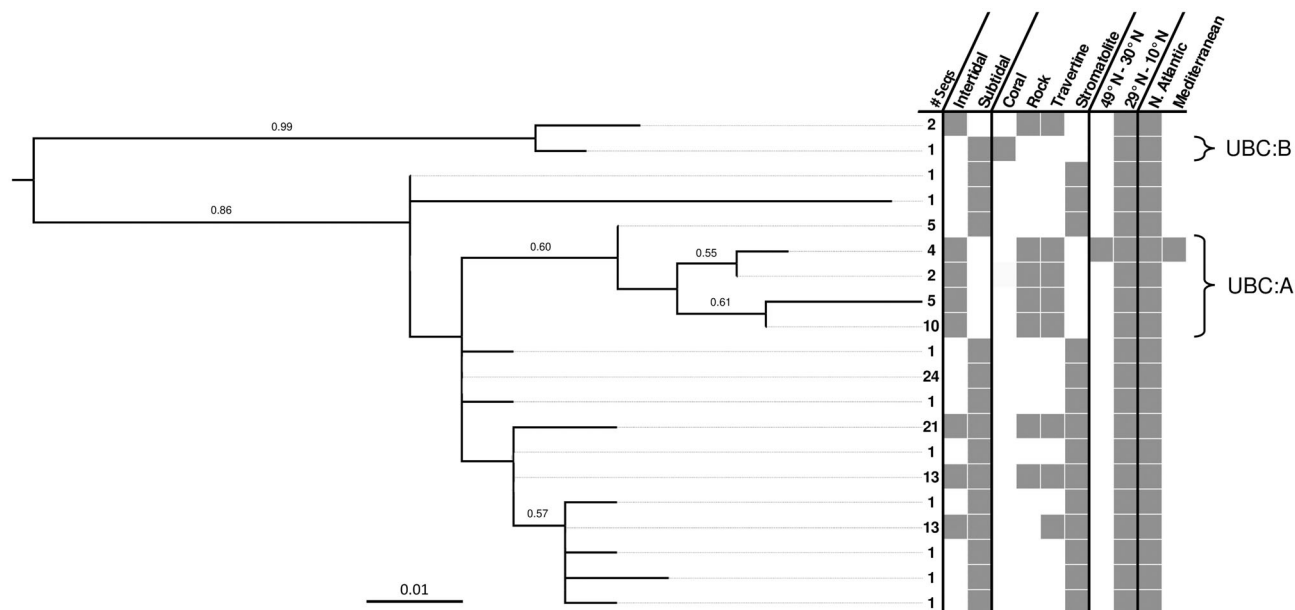


FIG. 6. Maximum likelihood phylogenetic tree (1000 bootstraps using the GTRGAMMA substitution model) of 16S rRNA sequences from 32 previously published studies and novel data collected for this study placed within the euendolith “unknown boring cluster” (UBC) using the Cydrasil 2.0 protocol. The UBC:A branch was almost exclusively observed in intertidal travertine and rock samples and UBC:B detected only on coral. The tree was rooted to the nearest outgroup on the Cydrasil reference tree. Shaded cells on the right indicate the presence of that ASV in different habitats, host substrata, latitude, and ocean categories. # Seqs indicates the number of studies that contained the ASV, and the scale bar denotes nucleotide substitution per site.

cyanobacterial families that were almost ubiquitous over all samples analyzed.

In terms of sequence identification using the SILVA database for ASVs falling within the clusters identified by Roush et al. (2020), sequences placed within the euendolith Cluster 1 (the *Leptolynghya*-like group) comprised the Nodosilineaceae and the Phormidiesmiaceae and may also include the well-documented euendolith *Plectonema terebrans* (Roush and Garcia-Pichel 2020). Cluster 2, the Pleurocapsalean group, is a diverse group that encompasses known euendoliths including *Hyella* sp., *Solentia* sp., and *Hormathonema* sp. which fall within the Xenococcaceae. The UBC cluster is a cryptic group whose closest alignment is to the Xenococcaceae (Roush and Garcia-Pichel 2020); however, further investigation is necessary to classify the group. Sequences that were placed within Cluster 3, the *Mastigocoleus testarum*-like group, were contained in the Nostocaceae, the family that includes the known euendoliths *Kyrtuthrix dalmatica* (Palinska et al. 2017, Ndhlovu et al. 2019) and *Scytonema endolithicum* (Gektidis et al. 2007). It is worth noting that the euendolith clusters from Roush et al. (2020), used to guide this study introduce a bias to the dataset that should be recognized; the clusters were determined from research focused on intertidal rock and travertine tiles in the Caribbean.

Distribution of Euendolithic cyanobacteria. The second objective was to examine the distribution of the euendoliths. This analysis revealed that all clusters

were present in temperate marine systems, on rock, travertine, coral, shell, and coralline algae.

Neither latitudinal gradients nor ocean connectivity/proximity was informative in explaining the presence of the euendolith cluster across the biogeographic regions. For example, the UBC cluster was notably absent from several geographical categories, with no obvious pattern to its absence. The Pleurocapsalean cluster and the UBC were both absent from the latitudinal category of 9° N–10° S despite this containing five studies that included samples from coral, coralline algae, and rock, in all of which the UBC cluster was found elsewhere at other latitudes (Fig. 5). The UBC cluster was a relatively small group with fewer occurrences and lower diversity than other clusters (Fig. 6), which suggests a relatively new group that has not diversified to have the greater temperature and substratum specificity shown by other clusters.

The UBC and the Pleurocapsalean cluster were notably absent from equatorial marine samples, possibly as a result of a sampling bias toward more active grazing species in the case of the Pleurocapsalean cluster (Grange et al. 2015) and sampling of more mature euendolith communities (Roush and Garcia-Pichel 2020). Nevertheless, their presence in equatorial samples was expected. Some euendolithic species are more easily removed by grazing, such as *Hyella* sp. (contained within the Pleurocapsalean cluster) and *Mastigocoleus testarum* (Grange et al. 2015) due to their shallow boring or poor

attachment. These genera were also absent from echinoderms and polychaete tubes, and the Pleurocapsalean cluster was only absent from chitons. This may be explained by high grazing activity on those substrata by other organisms, or self-cleaning by the organism, which may remove weakly attached bacteria, allowing deeper borers, or cyanobacteria with greater attachment strength, to persist.

The absence of any geographic trends in endolith distribution among oceans or latitudes is presumably a result of the width of the latitudinal brackets used, while oceans include many habitats and bioregions with a wide range of conditions of light intensity and temperature. However, using ocean as a metadata category for the phylogenetic trees of individual clusters allowed the observation of ASVs that were detected more widely than others. For example, the “Ocean” categories demonstrate the larger geographical distribution better than “Latitude” for the branches within the phylogenetic trees.

Of particular interest was the genetic diversity analysis of the UBC. Over half of the ASVs were identified in stromatolites, with half found exclusively there. The topography of the tree suggests stromatolites as an evolutionary origin for the cluster, with UBC:A (Fig. 6) diverging from stromatolites and being identified exclusively in rock and travertine. The single ASV observed in corals in the North Atlantic is particularly interesting, as it could represent radiation of this recently discovered group into corals as a new substratum, making it of future concern over coral reef degradation should it disperse to other latitudes and geographical areas. Where present, the UBC is an important pioneer cluster in euendolith colonization dynamics (Roush and Garcia-Pichel 2020), so it would be of interest to further investigate the identity, origin, and geographical expansion of the cluster.

The cyanobacterial community was most similar among coralline algae, shells, coral, and rock (including travertine), and these substrata collectively contained all the previously identified euendolith clusters. ASVs tended to be quite substratum-specific, usually being restricted to either rock and/or travertine and one other substratum, with very few being present in both coral and shell. This suggests high substratum (as well as geographic and niche) specificity of euendoliths, contrary to previous suggestions that phototrophic endoliths are generalists (Tribollet 2008, Marquet et al. 2013, Ndhlovu et al. 2019).

Although limited to a single study (Wenzel et al. 2018), no euendoliths were detected on isopod carapaces. Samples from isopods contained no photosynthetic cyanobacteria or other euendoliths. This could be a result of frequent molting of the isopods in the included study (*Jaera albifrons*) meaning the protective epicuticle layer over the calcium carbonate layers does not become sufficiently eroded to allow euendolith communities to establish themselves.

Coralline algae, many shell-bearing organisms, and corals are important ecosystem engineers and are important for fostering biodiversity (Buschbaum et al. 2009, Gómez-Lemos et al. 2018). It is known that microbial dissolution of corals (Tribollet et al. 2009, Reyes-Nivia et al. 2013) and coralline algae (Reyes-Nivia et al. 2014) increases under conditions of elevated $p\text{CO}_2$. Consequently, changes in the identity and boring efficiency of the euendolithic communities associated with ecological engineers as a result of changes in ocean pH and temperature will have important effects on their fitness (Kaehler and McQuaid 1999), including the ability of corals to survive and recover from bleaching events (Pernice et al. 2020). This in turn is likely to lead to indirect cascading effects of climate change on the diverse communities that rely on them.

CONCLUSIONS

This analysis allowed the identification of a core euendolith microbiome, with cyanobacteria belonging to known euendolith clusters being ubiquitous; they were detected in both intertidal and subtidal habitats, in all oceans and in all bands of latitude included in the metastudy. In addition, euendoliths were observed in all host substrata with the exception of isopods, though these were represented by a single study. The *Leptolyngbya*-like cluster was detected in all habitats, substrata, and geographic locations, while the Pleurocapsalean cluster and *Mastigocoleus testarum*-like cluster were detected in the majority of these categories. This emphasizes the high diversity and ubiquitous nature of euendolithic cyanobacteria indicating high adaptability of euendoliths and therefore their potential to affect a wide range of globally important substrata and ecosystems. The biochemical changes expected in global aquatic systems with projected climate change favor the mechanisms of bioerosion by euendoliths, which may lead to increased community and ecosystem-level effects. The few studies that have examined the ecological effects of euendoliths in detail have highlighted both the threats and advantages that they can pose to their hosts (Kaehler and McQuaid 1999, Zardi et al. 2009, Ndhlovu et al. 2019), while the present study emphasizes their genetic diversity and specificity to substrata and bioregions. This makes an understanding of how host/endolith relations will alter under global climate change particularly challenging.

- Aldred, N. & Nelson, A. 2019. Microbiome acquisition during larval settlement of the barnacle *Semibalanus balanoides*. *Biol. Lett.* 15:20180763.
- Amir, A., McDonald, D., Navas-Molina, J., Kopylova, E., Morton, J. T., Zech Xu, Z., Kightley, E. P., Thompson, L. R., Hyde, E. R., Gonzalez, A. & Knight, R. 2017. Deblur rapidly resolves single-nucleotide community sequence patterns. *mSystems* 2:191.

- Arfken, A., Song, B., Bowman, J. S. & Piehler, M. 2017. Denitrification potential of the eastern oyster microbiome using a 16S rRNA gene based metabolic inference approach. *PLoS ONE* 12:e0185071.
- Banerjee, N. R., Furnes, H., Muehlenbachs, K., Staudigel, H. & de Wit, M. 2006. Preservation of ~3.4–3.5 ga microbial biomarkers in pillow lavas and hyaloclastites from the barberton greenstone belt, South Africa. *Earth Planet. Sci. Lett.* 241:707–22.
- Bolyen, E., Rideout, J. R., Dillon, M. R., Bokulich, N. A., Abnet, C. C., Al-Ghalith, G., Alexander, H. et al. 2019. Reproducible, interactive, scalable and extensible microbiome data science using QIIME 2. *Nat. Biotechnol.* 37:852–7.
- Brasier, M., McLoughlin, N., Green, O. & Wacey, D. 2006. A fresh look at the fossil evidence for early archaean cellular life. *Philos. Trans. R. Soc. Lond., B. Biol. Sci.* 361:887–902.
- Brito, A., Ramos, V., Seabra, R., Santos, A., Santos, C. L., Lopo, M., Ferreira, S. et al. 2012. Culture-dependent characterization of cyanobacterial diversity in the intertidal zones of the Portuguese coast: A polyphasic study. *Syst. Appl. Microbiol.* 35:110–9.
- Buschbaum, C., Dittmann, S., Hong, J., Hwang, I., Strasser, M., Thiel, M., Valdivia, N., Yoon, S. & Reise, K. 2009. Mytilid mussels: Global habitat engineers in coastal sediments. *Helgol. Mar. Res.* 63:47–58.
- Caldeira, K. & Berner, R. 1999. Seawater pH and atmospheric carbon dioxide. *Science* 286:2043.
- Caldeira, K. & Wickett, M. E. 2003. Anthropogenic carbon and ocean pH. *Nature* 425:365.
- Callahan, B. J., McMurdie, P. J., Rosen, M. J., Han, A. W., Johnson, A. J. A. & Holmes, S. P. 2016. DADA2: High-resolution sample inference from illumina amplicon data. *Nat. Methods* 13:581–3.
- Camacho, C., Coulouris, G., Avagyan, V., Ma, N., Papadopoulos, J., Bealer, K. & Madden, T. L. 2009. BLAST+: Architecture and applications. *BMC Bioinform.* 10:421.
- Cambers 2005. Caribbean islands, coastal ecology and geomorphology. In Schwartz, M. L. [Ed.] *Encyclopedia of Coastal Science*. Springer, Netherlands, Dordrecht, pp. 221–6.
- Campion-Alsumard, T. & Hutchings, P. 1995. Microbial endoliths in skeletons of live and dead corals: *Porites lobata* (Moorea, French Polynesia). *Mar. Ecol. Prog. Ser.* 117:149–57.
- Chacón, E., Berrendero, E. & Garcia Pichel, F. 2006. Biogeological signatures of endoboring cyanobacterial communities in marine carbonates from Cabo Rojo, Puerto Rico. *Sediment. Geol.* 185:215–28.
- Clarke, K. R. & Gorley, R. N. 2006. *PRIMER v6: User manual/tutorial*. PRIMER-E, Plymouth.
- Cleary, D. F. R., Swierds, T., Coelho, F. J. R. C., Polónia, A. R. M., Huang, Y. M., Ferreira, M. R. S., Putchakarn, S. et al. 2019. The sponge microbiome within the greater coral reef microbial metacommunity. *Nat. Commun.* 10:1644.
- Cockell, C. S. & Herrera, A. 2008. Why are some microorganisms boring? *Trends Microbiol.* 16:101–6.
- Couradeau, E., Roush, D., Guida, B. S. & Garcia-Pichel, F. 2017. Diversity and mineral substrate preference in endolithic microbial communities from marine intertidal outcrops (Isla de Mona, Puerto Rico). *Biogeosciences* 14:311–24.
- Ćurin, M., Peharda, M., Calcinai, B. & Golubić, S. 2014. Incidence of damaging endolith infestation of the edible mytilid bivalve *Modiolus barbatus*. *Mar. Biol. Res.* 10:179–89.
- Day, E. G., Branch, G. M. & Viljoen, C. 2000. How costly is molluscan shell erosion? A comparison of two patellid limpets with contrasting shell structures. *J. Exp. Mar. Biol. Ecol.* 243:185–208.
- De'ath, G., Lough, J. M. & Fabricius, K. E. 2009. Declining coral calcification on the great barrier reef. *Science* 323:116–9.
- Diaz, M., Piggot, A., Eberli, G. & Klaus, J. 2013. Bacterial community of oolitic carbonate sediments of the Bahamas archipelago. *Mar. Ecol. Prog. Ser.* 485: 9-24. *Mar. Ecol. Prog. Ser.* 485:9–24.
- Diaz-Pulido, G., Anthony, K., Kline, D., Dove, S. & Hoegh-Guldberg, O. 2011. Interactions between ocean acidification and warming on the mortality and dissolution of coralline algae. *J. Phycol.* 48:32–9.
- Donn, T. F. & Boardman, M. R. 1988. Bioerosion of rocky carbonate coastlines on Andros Island, Bahamas. *J. Coast. Res.* 4:381–94.
- Foster, J. S., Green, S. J., Ahrendt, S. R., Golubic, S., Reid, R. P., Hetherington, K. L. & Bebout, L. 2009. Molecular and morphological characterization of cyanobacterial diversity in the stromatolites of Highborne Cay, Bahamas. *ISME J.* 3:573–87.
- Garcia-Pichel, F., Ramírez-Reinat, E. & Gao, Q. 2010. Microbial excavation of solid carbonates powered by P-type ATPase-mediated transcellular Ca²⁺ transport. *Proc. Natl. Acad. Sci. USA.* 107:21749–54.
- Gazeau, F., Quiblier, C., Jansen, J. M., Gattuso, J., Middelburg, J. J. & Heip, C. H. R. 2007. Impact of elevated CO₂ on shellfish calcification. *Geophys. Res. Lett.* 34:L07603.
- Geist, J., Wunderlich, H. & Kuehn, R. 2008. Use of mollusc shells for DNA-based molecular analyses. *J. Moll. Stud.* 74:337–43.
- Gektidis, M., Dubinsky, Z. & Goffredo, S. 2007. Microendoliths of the shallow euphotic zone in open and shaded habitats at 30° N - Eilat, Israel - paleoecological implications. *Facies* 53:43–55.
- Gleason, F. H., Gadd, G. M., Pitt, J. I. & Larkum, A. W. D. 2017a. The roles of endolithic fungi in bioerosion and disease in marine ecosystems. II. potential facultatively parasitic anamorphic ascomycetes can cause disease in corals and molluscs. *Mycology* 8:216–27.
- Gleason, F. H., Gadd, G. M., Pitt, J. I. & Larkum, A. W. D. 2017b. The roles of endolithic fungi in bioerosion and disease in marine ecosystems. I. general concepts. *Mycology* 8:205–15.
- Godoy-Vitorino, F., Ruiz-Diaz, C., Rivera-Seda, A., Ramírez-Lugo, J. S. & Toledo-Hernández, C. 2017. The microbial biosphere of the coral *Acropora cervicornis* in northeastern Puerto Rico. *PeerJ* 5:e3717.
- Goldsmith, D. B., Pratte, Z. A., Kellogg, C. A., Snader, S. E. & Sharp, K. H. 2019. Stability of temperate coral *Astrangia poculata* microbiome is reflected across different sequencing methodologies. *AIMS Microbiol.* 5:62–76.
- Golubic, S., Friedmann, E. I. & Schneider, J. 1981. The lithobiontic ecological niche, with special reference to microorganisms. *J. Sediment. Res.* 51:475–8.
- Gómez-Lemos, L. A., Doropoulos, C., Bayraktarov, E. & Diaz-Pulido, G. 2018. Coralline algal metabolites induce settlement and mediate the inductive effect of epiphytic microbes on coral larvae. *Sci. Rep.* 8:17557.
- Grange, J., Rybarczyk, H. & Tribollet, A. 2015. The three steps of the carbonate biogenic dissolution process by microborers in coral reefs (New Caledonia). *Environ. Sci. Pollut. Res. Int* 22:13625–37.
- Guida, B. S., Bose, M. & Garcia-Pichel, F. 2017. Carbon fixation from mineral carbonates. *Nat. Commun.* 8:1025.
- Guida, B. S. & Garcia-Pichel, F. 2016. Extreme cellular adaptations and cell differentiation required by a cyanobacterium for carbonate excavation. *Proc. Natl. Acad. Sci. USA* 113:5712–7.
- Havemann, S. A. & Foster, J. S. 2008. Comparative characterization of the microbial diversities of an artificial microbialite model and a natural stromatolite. *Appl. Environ. Microbiol.* 74:7410–21.
- Hogan, B., Costantini, F. & Lacy, E. 1986. *Manipulating the mouse embryo: A laboratory manual*. Cold Spring Harbor, New York, Cold Spring Harbor Laboratory Press, 814 pp.
- Hurd, C. L., Beardall, J., Comeau, S., Cornwall, C. E., Havenhand, J. N., Munday, P. L., Parker, L. M., Raven, J. A. & McGraw, C. M. 2020. Ocean acidification as a multiple driver: How interactions between changing seawater carbonate parameters affect marine life. *Mar. Freshw. Res.* 71:263–74.
- Kaehler, S. & McQuaid, C. D. 1999. Lethal and sub-lethal effects of phototrophic endoliths attacking the shell of the intertidal mussel *Perna perna*. *Mar. Biol.* 135:497–503.
- Katoh, K. & Standley, D. M. 2013. MAFFT multiple sequence alignment software version 7: Improvements in performance and usability. *Mol. Biol. Evol.* 30:772–80.

- Kimes, N. E., Johnson, W. R., Torralba, M., Nelson, K. E., Weil, E. & Morris, P. J. 2013. The *Montastraea faveolata* microbiome: Ecological and temporal influences on a Caribbean reef-building coral in decline. *Environ. Microbiol.* 15:2082–94.
- Klindworth, A., Pruesse, E., Schweer, T., Peplies, J., Quast, C., Horn, M. & Glöckner, F. O. 2013. Evaluation of general 16S ribosomal RNA gene PCR primers for classical and next-generation sequencing-based diversity studies. *Nucleic Acids Res.* 41:e1.
- Knoll, A. H., Golubic, S., Green, J. & Swett, K. 1986. Organically preserved microbial endoliths from the late proterozoic of east Greenland. *Nature* 321:856–7.
- Kumar, S., Stecher, G. & Tamura, K. 2016. MEGA7: Molecular evolutionary genetics analysis version 7.0 for bigger datasets. *Mol. Biol. Evol.* 33:1870–4.
- Leticia, I. & Bork, P. 2019. Interactive tree of life (iTOL) v4: Recent updates and new developments. *Nucleic Acids Res.* 47: W256–9.
- Li, J., Chen, Q., Zhang, S., Huang, H., Yang, J., Tian, X. & Long, L. 2013. Highly heterogeneous bacterial communities associated with the south China sea reef corals *Porites lutea*, *Galaxea fuscicularis* and *Acropora millepora*. *PLoS ONE* 8:e71301.
- Marcelino, V. R., Morrow, K. M., van Oppen, M. J. H., Bourne, D. G. & Verbruggen, H. 2017. Diversity and stability of coral endolithic microbial communities at a naturally high pCO₂ reef. *Mol. Ecol.* 26:5344–57.
- Marcelino, V. R. & Verbruggen, H. 2016. Multi-marker metabarcoding of coral skeletons reveals a rich microbiome and diverse evolutionary origins of endolithic algae. *Sci. Rep.* 6:31508.
- Marquet, N., Nicastro, K. R., Gektidis, M., McQuaid, C. D., Pearson, G. A., Serrão, E. A. & Zardi, G. I. 2013. Comparison of phototrophic shell-degrading endoliths in invasive and native populations of the intertidal mussel *Mytilus galloprovincialis*. *Biol. Invasions* 15:1253–72.
- Melzner, F., Stange, P., Trübenbach, K., Thomsen, J. Ö., Casties, I., Panknin, U., Gorb, S. N. & Gutowska, M. A. 2011. Food supply and seawater pCO₂ impact calcification and internal shell dissolution in the blue mussel *Mytilus edulis*. *PLoS ONE* 6:e24223.
- Murphy, G. N., Perry, C. T., Chin, P. & McCoy, C. 2016. New approaches to quantifying bioerosion by endolithic sponge populations: Applications to the coral reefs of Grand Cayman. *Coral Reefs* 35:1109–21.
- Ndhlovu, A., McQuaid, C. D., Nicastro, K., Maquet, N., Gektidis, M., Mobaco, C. J. & Zardi, G. 2019. Biogeographical patterns of endolithic infestation in an invasive and an indigenous intertidal marine ecosystem engineer. *Diversity* 11:75.
- Orr, J. C., Fabry, V. J., Aumont, O., Bopp, L., Doney, S. C., Feely, R. A., Gnanadesikan, A. et al. 2005. Anthropogenic ocean acidification over the twenty-first century and its impact on calcifying organisms. *Nature* 437:681–6.
- Palinska, K., Abed, R., Vogt, J., Radtke, G. & Golubic, S. 2017. Microbial endoliths on east adriatic limestone coast: Morphological vs. molecular diversity. *Geomicrobiol. J.* 34:903–15.
- Partensky, F., Hess, W. R. & Vault, D. 1999. Prochlorococcus, a marine photosynthetic prokaryote of global significance. *Microbiol. Mol. Biol. Rev.* 63:106–27.
- Pernice, M., Raina, J., Rädicker, N., Cárdenas, A., Pogoreutz, C. & Voolstra, C. R. 2020. Down to the bone: The role of overlooked endolithic microbiomes in reef coral health. *ISME J.* 14:325–34.
- Pfister, C. A., Meyer, F. & Antonopoulos, D. A. 2010. Metagenomic profiling of a microbial assemblage associated with the californian mussel: A node in networks of carbon and nitrogen cycling. *PLoS ONE* 5:e10518.
- Pollock, F. J., McMinds, R., Smith, S., Bourne, D. G., Willis, B. L., Medina, M., Thurber, R. V. & Zaneveld, J. R. 2018. Coral-associated bacteria demonstrate phyllosymbiosis and copolygeny. *Nat. Commun.* 9:4921.
- Price, M. N., Dehal, P. S. & Arkin, A. P. 2010. FastTree 2 – approximately maximum-likelihood trees for large alignments. *PLoS ONE* 5:e9490.
- Prusina, I., Peharda, M., Ezgeta-Balic, D., Puljas, S., Glamuzina, B. & Golubic, S. 2015. Life-history trait of the mediterranean keystone species *Patella rustica*: Growth and microbial bioerosion. *Mediterr. Mar. Sci.* 16:2.
- Quast, C., Pruesse, E., Yilmaz, P., Gerken, J., Schweer, T., Yarza, P., Peplies, J. Ö. & Glöckner, F. O. 2013. The SILVA ribosomal RNA gene database project: Improved data processing and web-based tools. *Nucleic Acids Res.* 41:D590–6.
- Quéré, G., Intertaglia, L., Payri, C. & Galand, P. E. 2019. Disease specific bacterial communities in a coralline algae of the northwestern Mediterranean sea: A combined culture dependent and -independent approach. *Front. Microbiol.* 10:1850.
- Rambaut, A. 2012. FigTree V1.4. Accessed November 14, 2022.
- Ramírez-Reinat, E. & Garcia-Pichel, F. 2012a. Prevalence of Ca²⁺-ATPase-mediated carbonate dissolution among cyanobacterial euendoliths. *Appl. Environ. Microbiol.* 78:7–13.
- Ramírez-Reinat, E. L. & Garcia-Pichel, F. 2012b. Characterization of a marine cyanobacterium that bores into carbonates and the redescription of the genus *Mastigocoleus*. *J. Phycol.* 48:740–9.
- Reyes-Nivia, C., Diaz-Pulido, G., Kline, D., Guldberg, O. & Dove, S. 2013. Ocean acidification and warming scenarios increase microbioerosion of coral skeletons. *Glob. Change Biol.* 19:1919–29.
- Reyes-Nivia, M., Diaz-Pulido, G. & Dove, S. 2014. Relative roles of endolithic algae and carbonate chemistry variability in the skeletal dissolution of crustose coralline algae. *Biogeosci. Discuss.* 11:4615–26.
- Rodolfo-Metalpa, R., Houlbrèque, F., Tambutté, É., Boisson, F., Baggini, C., Patti, F. P., Jeffree, R., Fine, M., Foggo, A., Gattuso, J. & Hall-Spencer, J. 2011. Coral and mollusc resistance to ocean acidification adversely affected by warming. *Nat. Clim. Change* 1:308–12.
- Roush, D., Couradeau, E., Guida, B., Neuer, S. & Garcia-Pichel, F. 2018. A new niche for anoxygenic phototrophs as endoliths. *Appl. Environ. Microbiol.* 84:2055.
- Roush, D. & Garcia-Pichel, F. 2020. Succession and colonization dynamics of endolithic phototrophs within intertidal carbonates. *Microorganisms* 8:214.
- Roush, D., Giraldo-Silva, A. & Garcia-Pichel, F. 2021. Cydrasil 3, a curated 16S rRNA gene reference package and web app for cyanobacterial phylogenetic placement. *Sci. Data* 8:230.
- Rubio-Portillo, E., Santos, F., Martínez-García, M., de Los Ríos, A., Ascaso, C., Souza-Egipsy, V., Ramos-Esplá, A. A. & Anton, J. 2016. Structure and temporal dynamics of the bacterial communities associated to microhabitats of the coral *Oculina patagonica*. *Environ. Microbiol.* 18:4564–78.
- Schneider, J. & Le Campion-Alsumard, T. 1999. Construction and destruction of carbonates by marine and freshwater cyanobacteria. *Eur. J. Phycol.* 34:417–26.
- Schönberg, C. & Wisshak, M. 2012. The perks of being endolithic. *Aquat. Biol.* 17:1–5.
- Schönberg, C. H. L., Fang, J. K. H., Carreiro-Silva, M., Tribollet, A. & Wisshak, M. 2017. Bioerosion: The other ocean acidification problem. *ICES J. Mar. Sci.* 74:895–925.
- Schöttner, S., Pfitzner, B., Grünke, S., Rasheed, M., Wild, C. & Ramette, A. 2011. Drivers of bacterial diversity dynamics in permeable carbonate and silicate coral reef sands from the red sea. *Environ. Microbiol.* 13:1815–26.
- Sharp, K. H., Pratte, Z. A., Kerwin, A. H., Rotjan, R. D. & Stewart, F. J. 2017. Season, but not symbiont state, drives microbiome structure in the temperate coral *Astrangia poculata*. *Microbiome* 5:120.
- Short, A. 2001. The distribution and impact of carbonate sands on southern australian beach-dune systems. In Robbins, L. L. & Magoon, O. T. [Eds.] *Carbonate Beaches 2000*. USGS and ASCE, Key Largo, Reston, VA, pp. 236–50.
- SRA Toolkit Development Team. 2020. SRA toolkit. <http://Ncbi.github.io/sra-tools/>.
- Stumpp, W. J., Melzner, F., Thorndyke, M. & Dupont, S. 2011. Seawater carbonate chemistry and filtering rate of *Strongylocentrotus purpuratus* during experiments. *PANGAEA*. <http://doi.org/10.1594/PANGAEA.774592>

- Sunagawa, S., DeSantis, T. Z., Piceno, Y. M., Brodie, E. L., DeSalvo, M. K., Voolstra, C. R., Weil, E., Andersen, G. L. & Medina, M. 2009. Bacterial diversity and white plague disease-associated community changes in the caribbean coral *Montastraea faveolata*. *ISME J.* 3:512–21.
- Sunagawa, S., Woodley, C. M. & Medina, M. 2010. Threatened corals provide underexplored microbial habitats. *PLoS ONE* 5:e9554.
- Tribollet, A. 2008. The boring microflora in modern coral reef ecosystems: A review of its roles. In Wisshak, M. & Tapanila, L. [Eds.] *Current Developments in Bioerosion*. Springer, Berlin Heidelberg, Berlin, Heidelberg, pp. 67–94.
- Tribollet, A., Godinot, C., Atkinson, M. & Langdon, C. 2009. Effects of elevated pCO₂ on dissolution of coral carbonates by microbial euendoliths. *Global Biogeochem. Cycles* 23:GB3008.
- Tribollet, A., Langdon, C., Golubic, S. & Atkinson, M. 2006. Endolithic microflora are major primary producers in dead carbonate substrates of Hawaiian coral reefs. *J. Phycol.* 42:292–303.
- Vijayan, N., Lema, K. A., Nedved, B. T. & Hadfield, M. G. 2019. Microbiomes of the polychaete *Hydroides elegans* (polychaeta: Serpulidae) across its life-history stages. *Mar. Biol.* 166:19.
- Webb, S. C. & Korrubel, J. L. 1994. Shell weakening in marine mytilids attributable to blue-green-alga *Mastigocoleus* sp. (nostochopsidaceae). *J. Shellfish. Res.* 13:11–7.
- Webster, N. S., Soo, R., Cobb, R. & Negri, A. P. 2011. Elevated seawater temperature causes a microbial shift on crustose coralline algae with implications for the recruitment of coral larvae. *ISME J.* 5:759–70.
- Wenzel, M. A., Douglas, A. & Piertney, S. B. 2018. Microbiome composition within a sympatric species complex of intertidal isopods (*Jaera albifrons*). *PLoS ONE* 13:e0202212.
- Williams, A., Brown, B., Putschim, L. & Sweet, M. 2015. Age-related shifts in bacterial diversity in a reef coral. *PLoS ONE* 10:e0144902.
- Zardi, G. I., Nicastro, K. R., McQuaid, C. D. & Gektidis, M. 2009. Effects of endolithic parasitism on invasive and indigenous mussels in a variable physical environment. *PLoS ONE* 4:e6560.
- Zhao, L., Shirai, K., Tanaka, K., Milano, S., Higuchi, T., Murakami-Sugihara, N., Walliser, E. O., Yang, F., Deng, Y. & Schöne, B. R. 2020. A review of transgenerational effects of ocean acidification on marine bivalves and their implications for sclerochronology. *Estuar. Coast. Shelf Sci.* 235:106620.

Supporting Information

Additional Supporting Information may be found in the online version of this article at the publisher's web site:

Figure S1. Alpha-rarefaction curves for host substrata (a), latitude category (b), habitat category (c), and ocean category (d) constructed using the number of unique ASVs and sequencing depth (number of sequences from all studies) of 16S rRNA sequences from 32 previously published studies and novel data collected for this study.

Figure S2. World map showing the position latitudinal categories used for the analysis of the global distribution of cyanobacterial species.

Figure S3. Maximum likelihood phylogenetic tree (1000 bootstraps using the GTRGAMMA substitution model) of 16S rRNA sequences from 32 previously published studies and novel data collected for this study placed within the euendolith cluster 1, *Leptolyngbya*-like cyanobacteria using the Cydrasil 2.0 protocol. The tree was rooted to the nearest outgroup on the Cydrasil reference tree. Shaded cells on the right indicate the presence of that ASV in different habitats, host substrata, latitude, and ocean categories. # Seqs indicates the number of studies that contained the ASV, and the scale bar denotes nucleotide substitution per site.

Figure S4. Maximum likelihood phylogenetic tree (1000 bootstraps using the GTRGAMMA substitution model) of 16S rRNA sequences from 32 previously published studies and novel data collected for this study placed within the euendolith cluster 2, the Pleurocapsales using the Cydrasil 2.0 protocol. The tree was rooted to the nearest outgroup on the Cydrasil reference tree. Shaded cells on the right indicate the presence of that ASV in different habitats, host substrata, latitude, and ocean categories. # Seqs indicates the number of studies that contained the ASV, and the scale bar denotes nucleotide substitution per site.

Figure S5. Maximum likelihood phylogenetic tree (1000 bootstraps using the GTRGAMMA substitution model) of 16S rRNA sequences from 32 previously published studies and novel data collected for this study placed within the euendolith cluster 3, *Mastigocoleus testarum*-like cyanobacteria using the Cydrasil 2.0 protocol. The tree was rooted to the nearest outgroup on the Cydrasil reference tree. Shaded cells on the right indicate the presence of that ASV in different habitats, host substrata, latitude, and ocean categories. # Seqs indicates the number of studies that contained the ASV, and the scale bar denotes nucleotide substitution per site.